Published in final edited form as:
J Immunol. 2014 October 15; 193(8): 3925–3933. doi:10.4049/jimmunol.1400861.

IL-17A Enhances the Expression of Pro-fibrotic Genes through Upregulation of the TGF-β Receptor on Hepatic Stellate Cells in a JNK-dependent Manner

Thomas Fabre[*,‡], **Hassen Kared**[*], **Scott L. Friedman**[†], and **Naglaa H. Shoukry**[*,§]

[*]Centre de Recherche du Centre Hospitalier de l'Université de Montréal (CRCHUM), Montréal, QC, Canada

[†]Division of Liver Diseases, Icahn School of Medicine at Mount Sinai, New York, NY, USA

[‡]Département de microbiologie, infectiologie et immunologie, Université de Montréal, Montréal, QC, Canada

[§]Département de médecine, Faculté de médecine, Université de Montréal, Montréal, QC, Canada

Abstract

Activation of hepatic stellate cells (HSCs) is a key event in the initiation of liver fibrosis, characterized by enhanced extracellular matrix (ECM) production and altered degradation. Activation of HSCs can be modulated by cytokines produced by immune cells. Recent reports have implicated the pro-inflammatory cytokine IL-17A in liver fibrosis progression. We hypothesized that IL-17A may enhance activation of HSC and induction of the fibrogenic signals in these cells. The human HSC line LX2 and primary human HSCs were stimulated with increasing doses of IL-17A and compared to TGF-β and PBS-treated cells as positive and negative controls, respectively. IL-17A alone did not induce activation of HSC. However, IL-17A sensitized HSCs to the action of suboptimal doses of TGF-β as confirmed by strong induction of alpha-smooth muscle actin (α-SMA), collagen type I (COL1A1) and tissue inhibitor of matrix metalloproteinase I (TIMP-I) gene expression and protein production. IL-17A specifically upregulated the cell surface expression of TGF-β-RII following stimulation. Pretreatment of HSCs with IL-17A enhanced signaling through the TGF-β-RII as observed by increased phosphorylation of SMAD2/3 in response to stimulation with suboptimal doses of TGF-β. This enhanced TGF-β response of HSCs induced by IL-17A was JNK-dependent. Our results suggest a novel pro-fibrotic function for IL-17A by enhancing the response of HSCs to TGF-β through activation of the JNK pathway. IL-17A acts through upregulation and stabilization of the TGF-β-RII leading to increased SMAD2/3 signaling. These findings represent a novel example of cooperative signaling between an immune cytokine and a fibrogenic receptor.

Address correspondence and reprint requests to: Dr. Naglaa H. Shoukry, Centre de Recherche du CHUM, Tour Viger, Local R09.414, 900 rue St-Denis, Montréal, QC H2X 0A9, CANADA, Tel: (514) 890-8000 ext 35235, Fax: (514) 412-7936, Naglaa.shoukry@umontreal.ca.

Introduction

The activation of hepatic stellate cells (HSCs) is a key event in liver fibrosis (16). HSCs are activated by inflammatory signals, such as apoptotic bodies, reactive oxygen species (ROS) and cytokines released in the milieu, including transforming growth factor beta (TGF-β) which is considered the major pro-fibrotic cytokine (10, 34). Activated HSCs (aHSCs) undergo myoblastic transformation and upregulate alpha smooth muscle actin (α-SMA) expression. They produce increased amounts of extracellular matrix (ECM) components such as collagen type I and fibronectin (10). aHSCs also secrete matrix metalloproteinases (MMPs) that can degrade ECM (30) as well as tissue inhibitor of matrix metalloproteinase (TIMPs) (26). It is the imbalance between these two pathways that leads to the accumulation of collagen type I in the interstitial space of the liver and fibrosis.

TGF-β induces the activation of HSCs through the SMAD2/3 signaling pathway (12, 17). Phosphorylation of these SMADs leads to transcription of pro-fibrotic molecules and activation of other transcription factors associated with liver fibrosis progression. In the liver, TGF-β is mainly produced by activated macrophages, regulatory T cells (Tregs) and aHSCs in response to pro-inflammatory signals. Therefore, regulation of TGF-β metabolism and signaling pathways plays an important role in modulating liver fibrosis progression.

Liver fibrosis can also be modulated by innate and adaptive immunity directly through cell-cell interaction or indirectly *via* the secretion of cytokines (2). Individuals infected with human immunodeficiency virus (HIV) progress more rapidly to advanced stages of liver fibrosis and this progression correlates with the decline in CD4 T cell counts suggesting that CD4 T cells and the cytokines they produce may regulate activation of HSC. Indeed, Th1 cytokines like IFN-γ are anti-fibrotic whereas the Th2 cytokines IL-4 and IL-13 lead to direct HSC activation and enhance fibrosis by inducing TGF-β and platelet-derived growth factor (PDGF) secretion by macrophages (1, 2, 7). Furthermore, Tregs can induce the senescence of HSCs through IL-10 secretion and, therefore, are considered anti-fibrotic (25, 39, 40). However, the implication of other CD4 helper T cell populations is not well understood.

Th17 cells, a subpopulation of CD4 helper T cells, are important in mucosal immunity and defence against bacterial, viral and fungal pathogens. They develop from naïve CD4 T cells in response to the inflammatory cytokines IL-1β, IL-6, and TGF-β and require IL-23 to become fully mature effectors (5, 19). Th17 cells secrete pro-inflammatory cytokines such as IL-17A, IL-17F and TNF-α as well as the anti-inflammatory cytokine IL-22. IL-17 and IL-22 producing Th17 cells are enriched in the liver as compared to peripheral blood (3, 9). IL-17-producing cells were linked to liver fibrosis progression in different liver pathologies including alcoholic hepatitis and hepatitis B virus (HBV) infection (20, 38). IL-17A induces chemokine secretion by HSCs and hepatocytes, which include IL-8 and growth regulated protein alpha (GRO-α) that are important in the recruitment of pro-fibrotic macrophages, monocytes and neutrophils (20). Furthermore, signals induced by the IL-17 receptor complex IL-17RA/IL-17RC in different cell types, including HSCs, lead to activation of the intracellular factors NFκB, JNK, MAPK and STAT-3, which are all linked to inflammation and liver fibrosis progression (11, 18, 24, 31, 32). IL-17A also enhances liver fibrosis

through activation of macrophages leading to production of pro-fibrotic cytokines such as IL-6, TNF-α, TGF-β and PDGF (2, 37). Using IL-17RA$^{-/-}$ knockout mice, it was demonstrated *in vivo* that specific depletion of the IL-17RA on macrophages results in reduced liver fibrosis (37).

In this study, we have developed an *in vitro* fibrosis assay based on the quantification of pro-fibrotic markers α-SMA, collagen type I and TIMP-I produced by the hepatic stellate cell line (LX2) or primary human HSCs. This model was used to assess the molecular mechanisms and the direct fibrotic functions of IL-17A on HSCs. Using a combination of qRT-PCR, western blot, picro-Sirius red staining and flow cytometry, we have demonstrated that IL-17A has pro-fibrotic properties. This cytokine enhances the response of HSCs to the major pro-fibrotic cytokine TGF-β by upregulating the expression of the TGF-β-RII on the surface of HSCs in a JNK-dependent manner.

Materials and Methods

Antibodies

For flow cytometry, directly conjugated antibodies against TGF-β-RII-PE (R&D Systems, Minneapolis, MN) and CD217 (IL-17RA)-APC (clone 424LTS) (eBioscience, San Diego, CA) were used. For western blot, antibodies against the following molecules were used: TIMP-I (clone 2E7.1) (ABCAM, Cambridge, MA), MMP-2 (clone 6E3F8) (ABCAM, Toronto, ON), α-SMA (clone 1A4) (Sigma-Aldrich, St-Louis, MO), SMAD3 (clone C69H7) (Cell signaling Technology, Danvers, MA), Phospho-SMAD2/3 (clone C25A9) (Cell signaling Technology) and GAPDH (clone 6C5) (Santa Cruz Biotechnology, Inc, Santa Cruz, CA.).

Cell culture

The human HSC line LX2 and primary human HSCs were used as previously described (25). LX2 cells were cultured in Dulbecco's modified Eagle media (DMEM) (Wisent Inc, St-Bruno, QC) supplemented with 10% fetal bovine serum (FBS) (HyClone, Nepean, ON) and GlutaMAX™ (Life Technologies, Burlington, ON). For all experiments, LX2 cells were seeded at 2×10^4 cells/well in a 48-well plate, 2×10^5 cells/well in a 6-well plate or 1×10^5 cells/well in a 12-well plate. When cells reached 70% confluence, they were serum-starved in DMEM supplemented with GlutaMAX™ without FBS for 48 h prior to a 48 h stimulation in serum-free conditions.

Cytokines

Recombinant human IL-17A and TGF-β were obtained from R&D systems Inc.

Quantitative real-time RT-PCR

After stimulation, total RNA from the LX2 cells was extracted using the *realtime ready cell lysis kit* (Roche). cDNAs were generated with the *transcriptor universal cDNA* (Roche) kit with DNAse I treatment, then diluted in ultrapure water (Roche) at a ratio of 1:5 and amplified using the LightCycler® 480 SYBR Green I Master kit on a LightCycler® 480 (Roche). Relative expression of the pro-fibrotic genes ACTA2, COL1A1, TIMP-I and

TGFβ1 were measured and normalized to ribosomal 28s rRNA expression. Standard curves were generated for each gene, to determine the reaction efficiency. We used the advanced relative quantification method from Roche, according to this formula: efficacy of target gene $^{-\Delta Cp}$ / efficacy of housekeeping gene $^{-\Delta Cp}$. Primer sequences are listed in Table 1. TGFβ1 primers were purchased from Qiagen (Hs_TGFB1_1_SG QuantiTect Primer Assay)

Western blotting

After stimulation, cells were lysed with RIPA Buffer (NaCl, Nonidet N-40 (NP40), Sodium Dodecyl Sulfate (SDS), Tris-HCL buffer pH=8) in presence of protease and phosphatase inhibitors (Roche). For detection of α-SMA, MMP-2 and TIMP-I, 20μg of total proteins, quantified using a Bradford assay, were loaded on a 20% polyacrylamide gel, and then transferred onto a nitrocellulose membrane (Bio-Rad, Hercules, CA). For detection of SMAD2/3 and phospho-SMAD2/3, only 10μg of total proteins were used. Blots were incubated with primary antibody overnight at 4°C and then with secondary HRP-conjugated antibody (Cell Signaling Technology, Danvers, MA) at RT for 1h. Blots were developed with the ECLTM Prime Western Blotting Detection Reagent (GE Healthcare, Buckinghamshire, UK). GAPDH was used as a loading control.

Picro-Sirius red staining and immunofluorescence

5×10^5 LX2 cells were cultured in an 8 chamber slide (BD Biosciences, San José, CA), to 70% confluence. Cells were then serum-starved for 48 h followed by another 48 h stimulation in serum-free conditions. Collagen type I production was measured by picro-Sirius red staining. Where cells were fixed in an acetone bath at −20°C for 15 min. Slides were incubated for 1h in picro-Sirius red (Sigma-Aldrich, St-Louis, MO), washed 2 times in 0.05% glacial acetic acid. Sirius red quantification was performed on 3 different areas per condition using Adobe Photoshop CS4 (Adobe Systems Incorporated, San Jose, CA). For immunofluorescence, cells were fixed in a 20% acetone, 80% methanol bath at −20°C for 15 min. Slides were blocked in PBS 1% BSA for 1h then incubated 1h with anti-phospho-SMAD2/3 (clone C25A9) followed by a 1h incubation with goat anti-rabbit-Alexa-488 (Life Technologies). Slides were then mounted with ProLong® Gold Antifade Reagent with DAPI (Life Technologies). Images acquisition and analysis was performed on a Zeiss Axio Imager M2 using Zen software (Carl Zeiss Canada Ltd., Toronto, ON).

Flow cytometry analysis

LX2 cells were detached using Versene (Life technologies), washed twice in Fluorescence-activated Cell Sorting (FACS) buffer (PBS 1X, 1% FBS, 0.02% sodium azide) and incubated for 30 min incubation with the antibodies. Cells were then washed in FACS buffer and fixed with fixation buffer (PBS 1X, 1% Formaldehyde). Data acquisition was performed on a BD-LSRII equipped with blue (488nm), red (633nm) and violet (405nm) lasers using FACSDIVA software (version 5.0.3) (BD Biosciences). FACS analysis was performed on FlowJo software (version 9.4.11) for Mac (Tree Star, Ashland, OR).

Statistical analysis

All data were analysed using GraphPad Prisms 5 (GraphPad Software, La Jolla, CA) and differences between the means for each condition were evaluated by a one-way ANOVA followed by a Tukey post hoc test.

Results

IL-17A synergizes with TGF-β to induce hepatic stellate cell activation

To evaluate the effect of IL-17A on HSCs, we stimulated LX2 cells for 48h with a low dose of 1 ng/mL and a high non-physiological dose of 40 ng/mL of IL-17A (referred to hereafter as IL-17A^{lo} and IL-17A^{hi}, respectively). Cells stimulated with TGF-β or PBS were used as positive and negative controls, respectively. Using a range from 0.1 to 10ng/mL, we determined that TGF-β induced a plateau of activation at 2.5 ng/mL (referred to as TGF-β^{hi}) (data not shown). We also tried different times of stimulation (4 h and 24 h) but we have observed significant changes only at 48 h of stimulation (Data not shown). TGF-β^{hi} induced a 5-fold increase in the expression of COL1A1 (collagen type I), ACTA2 (α-SMA) and TIMP-I genes as compared to PBS-treated cells (n=3, $p<0.0001$) (Figure 1A). Increased production of α-SMA and TIMP-I proteins was also observed by western blot (Figure 1B). Similarly, picro-Sirius red staining showed a 4-fold increase in collagen type I production in the TGF-β^{hi}-treated as compared to the PBS-treated LX2 cells (n=3, $p<0.05$) (Figure 1D and F). We also used a suboptimal dose of TGF-β (0.5 ng/mL), referred to as TGF-β^{lo}, that induces intermediate activation of HSC with a 2-fold increase in COL1A1 (n=3, $p<0.001$) and TIMP-I (n=3, $p<0.05$) mRNA. This dose also induced low levels of α-SMA protein as measured by western blot, and weak picro-Sirius red staining. IL-17A alone, at both low and high doses, was insufficient to activate LX2 cells. No significant increase in pro-fibrotic markers was observed as compared to PBS-treated cells at neither the mRNA (Figure 1A) nor the protein level (Figure 1B, D and F). IL-17A at both doses induced strong expression of TGF-β1 gene (Supplementary Figure S1), as previously described (24, 35). Similar results were observed with shorter stimulation time (Data not shown). However, we observed strong activation of LX2 cells, similar to TGF-β^{hi}, when IL-17A was combined with a suboptimal TGF-β^{lo} dose. A 5-fold increase in COL1A1 (n=3, $p<0.0001$), ACTA2 (n=3, $p<0.0001$) and TIMP-I (n=3, $p<0.0001$) expression was measured by qRT-PCR when compared to PBS-treated cells. Furthermore, an increase of over 2-fold (n=3, $p<0.0001$, represented by white asterisks) was observed when compared to TGF-β^{lo} alone (Figure 1A). These transcription profiles were validated at the protein level. A strong production of α-SMA and TIMP-I was observed by western blot in LX2 cells treated with IL-17A and TGF-β^{lo} (Figure 1B). Finally, collagen type I production was also higher (n=3, $p<0.05$) when compared to both TGF-β^{lo}- and PBS-treated LX2 cells (Figure 1D and F). Altogether these results suggest that IL-17A alone is not sufficient to prime LX2 cell activation. However, this cytokine can act in synergy with TGF-β to induce the fibrogenic process.

IL-17A pro-fibrotic function is validated in primary human hepatic stellate cells

Next, we validated our results using primary human HSCs. Similar to previous reports, TIMP-I and MMP-2 expression were higher by primary HSCs than LX2 cells (36). IL-17A at both doses did not induce α-SMA, collagen type I, MMP-2 or TIMP-I. However, the

addition of IL-17A to suboptimal TGF-β^{lo} dose led to strong induction of α-SMA and TIMP-I (Figure 1C) observed by western blot, as compared to PBS- or TGF-β^{lo}- treated HSCs. picro-Sirius red staining demonstrated a similar effect on collagen type I production by primary HSCs (Figure 1E). However, these cells were more sensitive to TGF-β^{lo} than LX2 cells, as we observed a 3-fold increase in picro-Sirius red stain with TGF-β^{lo} alone. The addition of IL-17A to TGF-β^{lo} still induced a 5-fold increase in picro-Sirius red stain (Figure 1F) and was significantly higher than TGF-β^{lo} alone ($p<0.05$). Thus, our observations underscore again a synergetic effect between IL-17A and TGF-β, which validated our results obtained with the LX2 cell line.

Blockade of TGF-β receptor I and II-associated kinase abrogates the enhanced activation of HSCs by IL-17A and TGF-β

Next, we sought to determine if the IL-17A pro-fibrotic effect is mediated through increased response of HSCs to TGF-β. We used Ly2109761, a specific inhibitor of kinases associated to both the TGF-β-RI and TGF-β-RII subunits (23). This reagent interferes with TGF-β signaling by decreasing the phosphorylation of SMAD2/3 and has no effect on IL-17A signaling (Supplementary Figure S2). We determined the optimal concentration of Ly2109761 to be 100 μM (data not shown). The addition of Ly2019761 abrogated the transcription of COL1A1, ACTA2 and TIMP-I ($n=3$, $p<0.0001$), which is normally observed with the combination of IL-17A with TGF-β^{lo} stimulation (Figure 2A). Furthermore, COL1A1, ACTA2 and TIMP-I transcription was lower in the presence of the inhibitor than in PBS-treated cells. Inhibition of pro-fibrotic gene expression induced by Ly2109761 was higher than 95% (data not shown). These results were validated at the protein level by western blot. Upregulation of TIMP-I and α-SMA induced by IL-17A at both doses in combination with TGF-β^{lo} was lost by the addition of Ly2109761 (Figure 2B). Altogether, these results prove that TGF-β signaling is required for the enhancement of HSC activation observed in LX2 cells stimulated with IL-17A and suboptimal doses of TGF-β.

IL-17A induces the upregulation of TGF-β-RII expression on the surface of LX2 cells

We then explored the mechanisms by which IL-17A enhances response to TGF-β. First, we evaluated the cell surface expression of TGF-β-RII and IL-17RA upon cytokine stimulation. Flow cytometry analysis was performed on PBS-, IL-17A- and/or TGF-β-treated cells for 48 h. Summary of 5 independent experiments are presented as average fold change in the mean fluorescence intensity (MFI) between PBS- versus cytokine-stimulated cells. No significant variation in IL-17RA expression was observed ($n=5$, $p=0.243$) (Figure 3C) but the cell surface expression of TGF-β-RII was significantly altered ($n=5$, $p=0.0002$). TGF-β stimulation induced a decrease in TGF-β-RII cell surface expression which was significant at high but not at low doses ($n=5$, $p<0.05$) (Figure 3A and B). This indicates that LX2 cells respond to TGF-β, and through feedback mechanisms, downregulate the cell surface expression of its receptor. IL-17A upregulated the cell surface expression of TGF-β-RII when compared to PBS-treated HSCs ($n=5$, $p<0.01$) (Figure 3A and B). LPS-induced upregulation of TGF-β-RII was tested as a positive control and was similar to that of IL-17A (data not shown) (29). We also determined if IL-17A could prevent the downregulation of the TGF-β-RII expression induced by TGF-β. Therefore, we performed LX2 cell stimulation with TGF-β^{hi} and TGF-β^{lo} in combination with IL-17A. After 48 h of stimulation, IL-17A

significantly prevented downregulation of the TGF-β-RII induced by both doses of TGF-β ($n=5$, $p<0.05$) (Figure 3B). These results indicate that IL-17A can partially prevent TGF-β-RII downregulation induced by TGF-β and might lead to increased or sustained signaling.

IL-17A increases the phosphorylation of SMAD2/3 in response to suboptimal doses of TGF-β

In order to determine if the IL-17A-mediated upregulation of TGF-β-RII could enhance HSCs response to TGF-β, we evaluated if IL-17A could modulate the activation of the SMAD2/3 pathway. LX2 cells were stimulated for 24 h with or without IL-17A at both doses followed by 15 min stimulation with suboptimal TGF-β^{lo}. The phosphorylation of SMAD2/3 at serine 423/425 was evaluated by western blot, and compared to TGF-β^{hi}. No phosphorylation of SMAD2/3 was observed when cells were treated with IL-17A alone. A low, almost undetectable, level of phosphorylation was induced by TGF-β^{lo} as compared to TGF-β^{hi} (Figure 3D, left and right panels). However, similar to TGF-β^{hi}, robust phosphorylation of SMAD2/3 was observed in LX2 cells stimulated with IL-17A at both doses prior to exposure with TGF-β^{lo} (Figure 3D). The level of total SMAD2/3 was increased in LX2 cells treated with IL-17A^{hi}, which was not observed with IL-17A^{lo} (Figure 3D, right panel). We validated our results by confocal microscopy and observed increased phosphorylation of SMAD2/3 in TGF-β^{hi} and IL-17A prestimulated cells. However, the localization of SMAD2/3 was different with higher nuclear localization in IL-17A-stimulated cells (Figure 3E, Supplementary Figure S3A). These data correlate with the synergistic effect observed between IL-17A and TGF-β^{lo} (Figure 1), as well as the upregulation of TGF-β-RII cell surface expression induced by IL-17A (Figure 3A and B).

IL-17A enhances response of LX2 cells to TGF-β in a JNK-dependent manner

The increased nuclear localization of SMAD2/3 when HSCs were stimulated with IL-17A led us to investigate the activation of the JNK pathway. It was previously demonstrated that the activation of JNK enhances phosphorylation and nuclear translocation of SMAD2/3 leading to increased fibrosis (21, 33). We confirmed by western blot that IL-17A alone induces phosphorylation of JNK (Figure 4A). We next proceeded to inhibit the phosphorylation of JNK using the chemical inhibitor, SP600125 which was previously shown to inhibit liver fibrosis (4, 15, 18, 22). We determined the optimal concentration of SP600125 to be 10 μM (Data not shown). Blockade of the JNK pathway prevented the induction of pro-fibrotic gene expression (Data not shown) as well as protein production in response to IL-17A with suboptimal TGF-β^{lo} (Figure 4B). We also observed no significant variation in the gene expression profiles of COL1A1, ACTA2 and TIMP-I in LX2 cells stimulated with TGF-β alone in presence or absence of SP600125 (Data not shown). This suggests that SP600125 had no to little direct effect on the response to TGF-β itself. Moreover, inhibition of JNK blocked the upregulation of TGF-β-RII induced by IL-17A (Figure 4C and D). This observation correlated with a loss of increased phosphorylation of SMAD2/3, observed by western blot and immunofluorescence staining, after stimulation with IL-17A and suboptimal TGF-β^{lo} (Figure 4E and F, Supplementary Figure S3A, S3B). Interestingly, we observed by confocal microscopy, a low level of phosphorylated SMAD2/3 in IL-17A/TGF-β^{lo} stimulated HSCs, which was exclusively localized to the

cytoplasm. This suggests that IL-17A enhanced HSCs response to TGF-β by the activation of the JNK pathway.

Discussion

We have examined the pro-fibrogenic effect of IL-17A on both the LX2 cell line and primary human HSCs. We demonstrate that IL-17A alone was not sufficient to induce α-SMA, collagen type I and TIMP-I production. However, IL-17A enhanced stellate cell responses to TGF-β by increasing cell surface expression of its receptor which led to increased phosphorylation and nuclear translocation of the transcription factors SMAD2/3 in response to suboptimal doses of TGF-β. Furthermore, we demonstrated that this phenotype was dependent on the activation of the JNK pathway by IL-17A.

We also investigated if IL-17A can directly induce pro-fibrotic genes within HSCs. We demonstrated that IL-17 could not induce COL1A1, ACTA2 and TIMP-I gene or protein expression in LX2 cells or primary human HSCs. These results differ from recent reports suggesting that IL-17A can directly enhance the transcription of pro-fibrotic genes in HSCs (24, 32). However, these two studies attributed this function to two different pathways (MAPK or STAT3). These discrepancies could also be explained by differences in the experimental conditions. In these two reports, the authors stimulated HSCs for 2–8 h which in our hands did not show any effect (Data not shown). This is why we chose to stimulate our cells for 48 h based on a previous report showing that efficient IL-17A signaling is observed after a minimum of 24 h (42). Furthermore, we performed all stimulations on serum-starved cells in order to eliminate the presence of TGF-β found in FBS. On the other hand, our results are concordant with other groups that demonstrated that IL-17A did not induce the expression of pro-fibrotic genes but rather the expression of pro-inflammatory cytokines and chemokines involved in the recruitment of macrophages, neutrophils and monocytes (13, 20, 37). Dermal fibroblasts were also reported to produce pro-inflammatory cytokines and chemokines in response to IL-17A without producing pro-fibrotic molecules such as collagen type I (6).

IL17A can also enhance fibrosis indirectly by inducing expression of TGF-β1 (24, 35). We also observed that IL-17A induces TGF-β1 expression in a dose-dependent manner on LX2 cells which suggest complementary effect of those two cytokines. In mice, specific knockdown of IL-17RA on macrophages strongly reduced liver fibrosis, whereas modest reduction was observed if knockdown is performed on liver resident cells (37). Indeed, IL-17A can induce the production of the two major pro-fibrotic cytokines PDGF and TGF-β with other inflammatory cytokines IL-1β, IL-6 and TNF-α by macrophages, neutrophils and monocytes (2, 13, 20). Furthermore, inflammatory cytokines during hepatitis lead to activation of dendritic cells (DCs) and monocytes. Activated DCs and monocytes then secrete key cytokines involved in the differentiation and activation of Th17 cells. Finally, liver inflammation leads not only to cytokine production but also to increased chemokine production by activated DCs, monocytes and hepatocytes, such as CCL20, CCL22 and CCL17, which are involved in the recruitment of Th17 cells to the liver (14). This suggests a possible interaction between IL-17A and TGF-β-producing cells and requires further investigation in in vivo models of fibrosis.

We demonstrated that IL-17A enhances the response of both LX2 cells and primary human HSCs to suboptimal doses of TGF-β. We observed robust production of pro-fibrotic genes after stimulation of HSCs with IL-17A in combination with TGF-β suggesting a synergistic effect between those two cytokines. Blockade of TGF-β-R associated kinase prevented the induction of pro-fibrotic genes during IL-17A/TGF-β^{lo} stimulation which indicates that this phenotype is dependent on TGF-β signaling. The flow cytometry analysis of IL-17RA and TGF-β-RII showed that both receptors were expressed by HSCs. Cytokine stimulation did not affect the cell surface expression of IL-17RA. However, after IL-17A stimulation we observed increased cell surface expression of TGF-β-RII as well as prevention of its downregulation induced by TGF-β. It was also recently demonstrated that IL-17A increases PDGF-R expression in gut smooth muscle cells and may suggest that IL-17A can modulate expression of different growth factor receptor (27). In addition, we showed in IL-17A-stimulated HSCs increase phosphorylation and nuclear translocation of SMAD2/3 in response to suboptimal TGF-β. Thus, IL-17A is a pro-fibrotic cytokine that contributes to the regulation of the fibrogenic process by increasing the TGF-β response at several cellular levels in HSCs. Similar collaborations between two distinct signaling pathways were reported to enhance liver fibrosis and activation of HSCs (28). Altogether, these findings suggest that many interactions between fibrotic pathways are yet to be discovered.

The JNK pathway is one of the key fibrogenic and inflammatory pathways in the liver and can be activated by several cytokines including IL-17A (8, 11, 18, 22). JNK deficient mice exhibit reduced fibrosis after CCL4-treatment and purified HSCs from these mice are less responsive to activation signals (41). JNK plays an important role in regulating response to TGF-β through modulation of the phosphorylation and nuclear translocation of SMAD2/3 (21, 33). Furthermore, TGF-β itself induces late activation of JNK leading to a second round of activation of SMAD2/3 which correlates with increase fibrosis (33). We observed activation of JNK and increase nuclear translocation of SMAD2/3 in IL-17A-stimulated HSCs after only 15 min stimulation with TGF-β suggesting that IL-17A was responsible for this phenotype. Blocking JNK with a chemical inhibitor abrogated induction of pro-fibrotic genes, upregulation of the TGF-β-RII and increased phosphorylation of SMAD2/3 after IL-17A with suboptimal TGF-β stimulation. Thus, IL-17A enhanced the response of HSCs to TGF-β in a JNK-dependent manner that may lead to increased fibrosis.

In conclusion, we have demonstrated that IL-17A is a pro-fibrotic cytokine with no direct fibrogenic effect on HSCs. However, IL-17A enhances the response of HSCs to TGF-β leading to increased production of collagen type I, α-SMA and TIMP-I. IL-17A may also enhance liver fibrosis indirectly via other mechanisms. First, it induces the recruitment of pro-inflammatory macrophages by increasing chemokine secretion by HSCs (20). IL-17A then activates these newly recruited macrophages to produce pro-fibrotic cytokines including TGF-β (24, 37). IL-17A also induces TGF-β by fibrotic cells including HSCs (24, 35). Finally, IL-17A enhances HSCs response to TGF-β by upregulating its receptor expression at the cell surface, in a JNK dependant manner, leading to increased fibrosis. Further studies should determine the interactions and cellular pathways involved in the cross-talk between TGF-β-producing cells, HSCs and IL-17A-producing cells, such as Th17, NK and NKT cells, during chronic hepatitis. Finally, functionnal characterization of

intrahepatic versus peripheral blood Th17 during liver injury and inflammation should be studied in order to validate our *in vitro* data.

Supplementary Material

Refer to Web version on PubMed Central for supplementary material.

Acknowledgments

This work was supported by grants from the Canadian Institutes for Health Research (CIHR) (HEO-115696) to NHS and The National Institutes of Health (NIH) (DK56621 and AA020709) to SLF. TF is the recipient of fellowships from the Fondation Gabriel Marquis, the Université de Montréal and the National CIHR Research Training Program on Hepatitis C (NCRTP-Hep C) and CIHR. NHS is the recipient of a Chercheur Boursier salary award from the Fonds de recherche du Québec - Santé (FRQ-S).

Abbreviations used in this article

α-SMA	alpha-smooth muscle actin
ACTA2	gene coding for alpha-smooth muscle actin
COL1A1	gene coding for collagen type I
ECM	extracellular matrix
HBV	Hepatitis B virus
HSCs	Hepatic stellate cells
MMPs	matrix metalloproteinases
PDGF	platelet-derived growth factor
TIMPs	tissue inhibitor of matrix metalloproteinase
Tregs	regulatory T cells

References

1. Baroni GS, D'Ambrosio L, Curto P, Casini A, Mancini R, Jezequel AM, Benedetti A. Interferon gamma decreases hepatic stellate cell activation and extracellular matrix deposition in rat liver fibrosis. Hepatology. 1996; 23:1189–1199. [PubMed: 8621153]
2. Barron L, Wynn TA. Fibrosis is regulated by Th2 and Th17 responses and by dynamic interactions between fibroblasts and macrophages. American journal of physiology. Gastrointestinal and liver physiology. 2011; 300:G723–728. [PubMed: 21292997]
3. Bengsch B, Seigel B, Flecken T, Wolanski J, Blum HE, Thimme R. Human Th17 cells express high levels of enzymatically active dipeptidylpeptidase IV (CD26). Journal of immunology (Baltimore, Md: 1950). 2012; 188:5438–5447.
4. Bennett BL, Sasaki DT, Murray BW, O'Leary EC, Sakata ST, Xu W, Leisten JC, Motiwala A, Pierce S, Satoh Y, Bhagwat SS, Manning AM, Anderson DW. SP600125, an anthrapyrazolone inhibitor of Jun N-terminal kinase. Proceedings of the National Academy of Sciences of the United States of America. 2001; 98:13681–13686. [PubMed: 11717429]
5. Bettelli E, Korn T, Oukka M, Kuchroo VK. Induction and effector functions of T(H)17 cells. Nature. 2008; 453:1051–1057. [PubMed: 18563156]
6. Brembilla N, Montanari E, Truchetet ME, Raschi E, Meroni P, Chizzolini C. Th17 cells favor inflammatory responses while inhibiting type I collagen deposition by dermal fibroblasts:

differential effects in healthy and systemic sclerosis fibroblasts. Arthritis research & therapy. 2013; 15:R151. [PubMed: 24289089]

7. Chiaramonte MG, Donaldson DD, Cheever AW, Wynn TA. An IL-13 inhibitor blocks the development of hepatic fibrosis during a T-helper type 2-dominated inflammatory response. The Journal of clinical investigation. 1999; 104:777–785. [PubMed: 10491413]
8. Das M, Sabio G, Jiang F, Rincon M, Flavell RA, Davis RJ. Induction of hepatitis by JNK-mediated expression of TNF-alpha. Cell. 2009; 136:249–260. [PubMed: 19167327]
9. Foster RG, Golden-Mason L, Rutebemberwa A, Rosen HR. Interleukin (IL)-17/IL-22-producing T cells enriched within the liver of patients with chronic hepatitis C viral (HCV) infection. Digestive diseases and sciences. 2012; 57:381–389. [PubMed: 22183819]
10. Friedman SL. Mechanisms of hepatic fibrogenesis. Gastroenterology. 2008; 134:1655–1669. [PubMed: 18471545]
11. Gaffen SL. Structure and signalling in the IL-17 receptor family. Nature reviews. Immunology. 2009; 9:556–567.
12. Greene RM, Nugent P, Mukhopadhyay P, Warner DR, Pisano MM. Intracellular dynamics of Smad-mediated TGFbeta signaling. Journal of cellular physiology. 2003; 197:261–271. [PubMed: 14502566]
13. Guillot A, Hamdaoui N, Bizy A, Zoltani K, Souktani R, Zafrani ES, Mallat A, Lotersztajn S, Lafdil F. Cannabinoid receptor 2 counteracts interleukin-17-induced immune and fibrogenic responses in mouse liver. Hepatology. 2013
14. Hammerich L, Heymann F, Tacke F. Role of IL-17 and Th17 cells in liver diseases. Clinical & developmental immunology. 2011; 2011:345803. [PubMed: 21197451]
15. Heo YS, Kim SK, Seo CI, Kim YK, Sung BJ, Lee HS, Lee JI, Park SY, Kim JH, Hwang KY, Hyun YL, Jeon YH, Ro S, Cho JM, Lee TG, Yang CH. Structural basis for the selective inhibition of JNK1 by the scaffolding protein JIP1 and SP600125. The EMBO journal. 2004; 23:2185–2195. [PubMed: 15141161]
16. Hernandez-Gea V, Friedman SL. Pathogenesis of liver fibrosis. Annual review of pathology. 2011; 6:425–456.
17. Inagaki Y, Okazaki I. Emerging insights into Transforming growth factor beta Smad signal in hepatic fibrogenesis. Gut. 2007; 56:284–292. [PubMed: 17303605]
18. Kluwe J, Pradere JP, Gwak GY, Mencin A, De Minicis S, Osterreicher CH, Colmenero J, Bataller R, Schwabe RF. Modulation of hepatic fibrosis by c-Jun-N-terminal kinase inhibition. Gastroenterology. 2010; 138:347–359. [PubMed: 19782079]
19. Korn T, Oukka M, Kuchroo V, Bettelli E. Th17 cells: effector T cells with inflammatory properties. Seminars in immunology. 2007; 19:362–371. [PubMed: 18035554]
20. Lemmers A, Moreno C, Gustot T, Marechal R, Degre D, Demetter P, de Nadai P, Geerts A, Quertinmont E, Vercruysse V, Le Moine O, Deviere J. The interleukin-17 pathway is involved in human alcoholic liver disease. Hepatology. 2009; 49:646–657. [PubMed: 19177575]
21. Liu Q, Zhang Y, Mao H, Chen W, Luo N, Zhou Q, Chen W, Yu X. A crosstalk between the Smad and JNK signaling in the TGF-beta-induced epithelial-mesenchymal transition in rat peritoneal mesothelial cells. PloS one. 2012; 7:e32009. [PubMed: 22384127]
22. Marra F, Delogu W, Petrai I, Pastacaldi S, Bonacchi A, Efsen E, Aleffi S, Bertolani C, Pinzani M, Gentilini P. Differential requirement of members of the MAPK family for CCL2 expression by hepatic stellate cells. American journal of physiology. Gastrointestinal and liver physiology. 2004; 287:G18–26. [PubMed: 15016614]
23. Melisi D, Ishiyama S, Sclabas GM, Fleming JB, Xia Q, Tortora G, Abbruzzese JL, Chiao PJ. LY2109761, a novel transforming growth factor beta receptor type I and type II dual inhibitor, as a therapeutic approach to suppressing pancreatic cancer metastasis. Molecular cancer therapeutics. 2008; 7:829–840. [PubMed: 18413796]
24. Meng F, Wang K, Aoyama T, Grivennikov SI, Paik Y, Scholten D, Cong M, Iwaisako K, Liu X, Zhang M, Osterreicher CH, Stickel F, Ley K, Brenner DA, Kisseleva T. Interleukin-17 signaling in inflammatory, Kupffer cells, and hepatic stellate cells exacerbates liver fibrosis in mice. Gastroenterology. 2012; 143:765–776. e761–763. [PubMed: 22687286]

25. Mentink-Kane MM, Cheever AW, Wilson MS, Madala SK, Beers LM, Ramalingam TR, Wynn TA. Accelerated and progressive and lethal liver fibrosis in mice that lack interleukin (IL)-10, IL-12p40, and IL-13Ralpha2. Gastroenterology. 2011; 141:2200–2209. [PubMed: 21864478]
26. Murphy G. Tissue inhibitors of metalloproteinases. Genome biology. 2011; 12:233. [PubMed: 22078297]
27. Nair DG, Miller KG, Lourenssen SR, Blennerhassett MG. Inflammatory cytokines promote growth of intestinal smooth muscle cells by induced expression of PDGF-Rbeta. Journal of cellular and molecular medicine. 2014; 18:444–454. [PubMed: 24417820]
28. Rozenfeld R, Gupta A, Gagnidze K, Lim MP, Gomes I, Lee-Ramos D, Nieto N, Devi LA. AT1R-CB(1)R heteromerization reveals a new mechanism for the pathogenic properties of angiotensin II. The EMBO journal. 2011; 30:2350–2363. [PubMed: 21540834]
29. Seki E, De Minicis S, Osterreicher CH, Kluwe J, Osawa Y, Brenner DA, Schwabe RF. TLR4 enhances TGF-beta signaling and hepatic fibrosis. Nature medicine. 2007; 13:1324–1332.
30. Siefert SA, Sarkar R. Matrix metalloproteinases in vascular physiology and disease. Vascular. 2012; 20:210–216. [PubMed: 22896663]
31. Sparna T, Retey J, Schmich K, Albrecht U, Naumann K, Gretz N, Fischer HP, Bode JG, Merfort I. Genome-wide comparison between IL-17 and combined TNF-alpha/IL-17 induced genes in primary murine hepatocytes. BMC genomics. 2010; 11:226. [PubMed: 20374638]
32. Tan Z, Qian X, Jiang R, Liu Q, Wang Y, Chen C, Wang X, Ryffel B, Sun B. IL-17A plays a critical role in the pathogenesis of liver fibrosis through hepatic stellate cell activation. Journal of immunology (Baltimore, Md: 1950). 2013; 191:1835–1844.
33. Wang XM, Zhang Y, Kim HP, Zhou Z, Feghali-Bostwick CA, Liu F, Ifedigbo E, Xu X, Oury TD, Kaminski N, Choi AM. Caveolin-1: a critical regulator of lung fibrosis in idiopathic pulmonary fibrosis. The Journal of experimental medicine. 2006; 203:2895–2906. [PubMed: 17178917]
34. Weng HL, Liu Y, Chen JL, Huang T, Xu LJ, Godoy P, Hu JH, Zhou C, Stickel F, Marx A, Bohle RM, Zimmer V, Lammert F, Mueller S, Gigou M, Samuel D, Mertens PR, Singer MV, Seitz HK, Dooley S. The etiology of liver damage imparts cytokines transforming growth factor beta1 or interleukin-13 as driving forces in fibrogenesis. Hepatology. 2009; 50:230–243. [PubMed: 19441105]
35. Wilson MS, Madala SK, Ramalingam TR, Gochuico BR, Rosas IO, Cheever AW, Wynn TA. Bleomycin and IL-1beta-mediated pulmonary fibrosis is IL-17A dependent. The Journal of experimental medicine. 2010; 207:535–552. [PubMed: 20176803]
36. Xu L, Hui AY, Albanis E, Arthur MJ, O'Byrne SM, Blaner WS, Mukherjee P, Friedman SL, Eng FJ. Human hepatic stellate cell lines, LX-1 and LX-2: new tools for analysis of hepatic fibrosis. Gut. 2005; 54:142–151. [PubMed: 15591520]
37. Yan S, Wang L, Liu N, Wang Y, Chu Y. Critical role of interleukin-17/interleukin-17 receptor axis in mediating Con A-induced hepatitis. Immunology and cell biology. 2012; 90:421–428. [PubMed: 21691280]
38. Zhang JY, Zhang Z, Lin F, Zou ZS, Xu RN, Jin L, Fu JL, Shi F, Shi M, Wang HF, Wang FS. Interleukin-17-producing CD4(+) T cells increase with severity of liver damage in patients with chronic hepatitis B. Hepatology. 2010; 51:81–91. [PubMed: 19842207]
39. Zhang L, Wang X, Zheng W, Shi M. The effects of interleukin-10 on the expression of Fas and FasL in rat hepatic stellate cells. Medicinal chemistry (Shariqah (United Arab Emirates)). 2006; 2:611–616. [PubMed: 17105443]
40. Zhang LJ, Zheng WD, Shi MN, Wang XZ. Effects of interleukin-10 on activation and apoptosis of hepatic stellate cells in fibrotic rat liver. World journal of gastroenterology : WJG. 2006; 12:1918–1923. [PubMed: 16609999]
41. Zhao G, Hatting M, Nevzorova YA, Peng J, Hu W, Boekschoten MV, Roskams T, Muller M, Gassler N, Liedtke C, Davis RJ, Cubero FJ, Trautwein C. Jnk1 in murine hepatic stellate cells is a crucial mediator of liver fibrogenesis. Gut. 2013
42. Zhao L, Tang Y, You Z, Wang Q, Liang S, Han X, Qiu D, Wei J, Liu Y, Shen L, Chen X, Peng Y, Li Z, Ma X. Interleukin-17 contributes to the pathogenesis of autoimmune hepatitis through inducing hepatic interleukin-6 expression. PloS one. 2011; 6:e18909. [PubMed: 21526159]

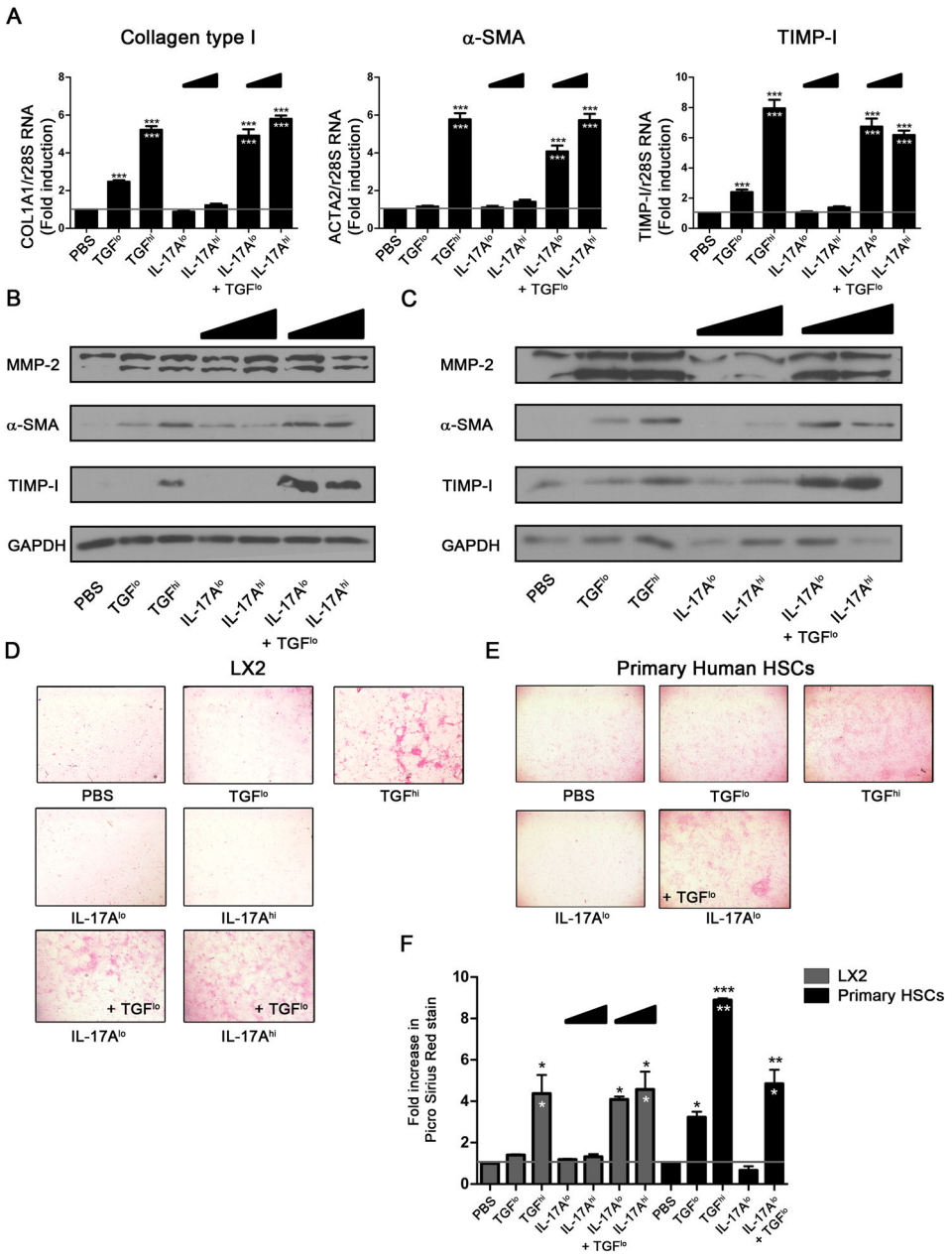

Figure 1. IL-17A enhances the fibrogenic process in LX2 and primary human hepatic stellate cells in response to TGF-β

(A) Relative expression of the pro-fibrotic genes: COL1A1, ACTA2 and TIMP-I by LX2 cells after 48 h stimulation with IL-17A ± TGF-β was determined by quantitative PCR, and results are shown as fold change compared PBS- versus cytokines-treated LX2 cells. Black stars represent a significant increase compared to PBS-treated cells whereas white stars represent a significant increase compared to cells treated with TGF-β at low dose. Protein expression of α-SMA, TIMP-I and MMP-2 after 48 h stimulation with IL-17A ± TGF-β was evaluated in LX2 (B) and primary human HSCs (C) by western blot. Collagen type I secretion was measured by Picro-Sirius red staining of LX2 (D) and primary human HSCs (E) after stimulation with IL-17A ± TGF-β, and relative quantification of Picro-Sirius red

staining was performed (F). Figure is representative of 3 independent experiments. One-way ANOVA was used followed by a Tukey post-test, *, $p<0.05$ **, $p<0.01$, *** $p<0.001$.

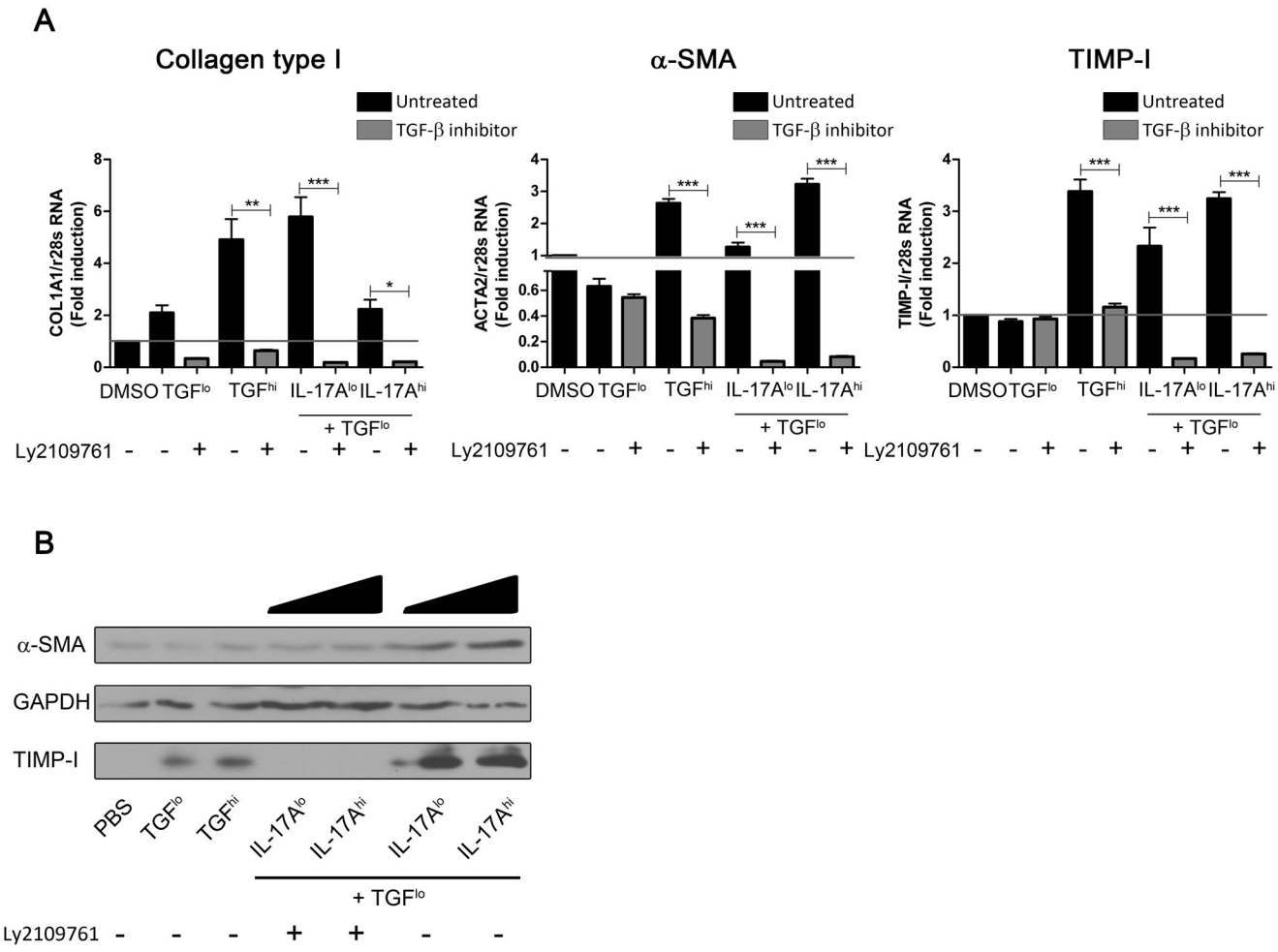

Figure 2. Blockade of TGF-β receptors associated kinase prevents increase response to TGF-β induced by IL-17A

Relative expression of the pro-fibrotic genes: COL1A1, ACTA2 and TIMP-I by LX2 cells after stimulation with IL-17A ± TGF-β, in presence or absence of the TGF-β receptors kinase inhibitors Ly2109761, was determined by quantitative RT-PCR, and results are shown as fold change compared PBS- versus cytokines-treated LX2 cells (A). Black bar charts represent conditions without Ly2109761 whereas grey bar charts represent conditions with Ly2109761. Ly2109761 prevents TIMP-I and α-SMA increased production induced by IL-17A + TGF-β^{lo}, as shown by western blot (B). One-way ANOVA was used followed by a Tukey post-test, *, $p<0.05$ **, $p<0.01$, *** $p<0.001$.

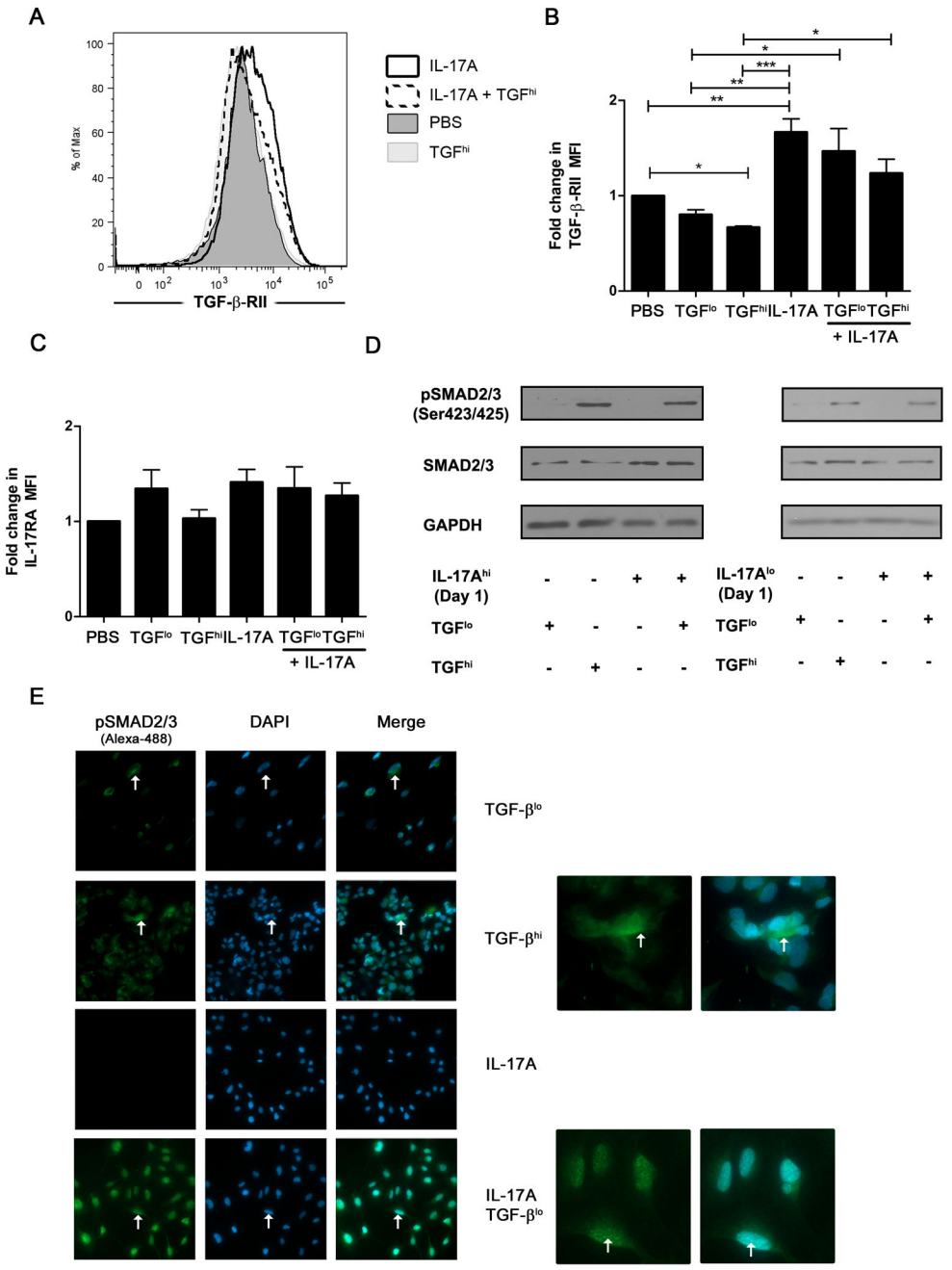

Figure 3. IL-17A increases TGF-β receptor cell surface expression and signaling on hepatic stellate cells

Cell surface expression of IL-17RA and TGF-β-RII was measured by flow cytometry after a 48 h stimulation with IL-17A and/or TGF-β. Representative histogram of TGF-β-RII cell surface expression induced by IL-17A and/or TGF-β stimulation (A). TGF-β-RII cell surface expression induced by IL-17A and/or TGF-β stimulation. Results are display as fold increase of MFI (n=5). (B). IL-17RA cell surface expression following IL-17A and/or TGF-β stimulation (C). Phosphorylation of SMAD2/3 at serine 423/425 was evaluated by western blot after a 15 min stimulation with TGF-β (D). Two colors immunofluorescence confocal

microscopy was used to observed phosphorylated SMAD2/3 (green, Alexa-488) and nucleus (Blue, DAPI) (E). Close up images are displayed for TGF-β^{hi} and IL-17A + TGF-β^{lo}. Panel D and E are representative of 3 independent experiments. One-way ANOVA was used followed by a Tukey post-test, *, $p<0.05$ **, $p<0.01$, *** $p<0.001$.

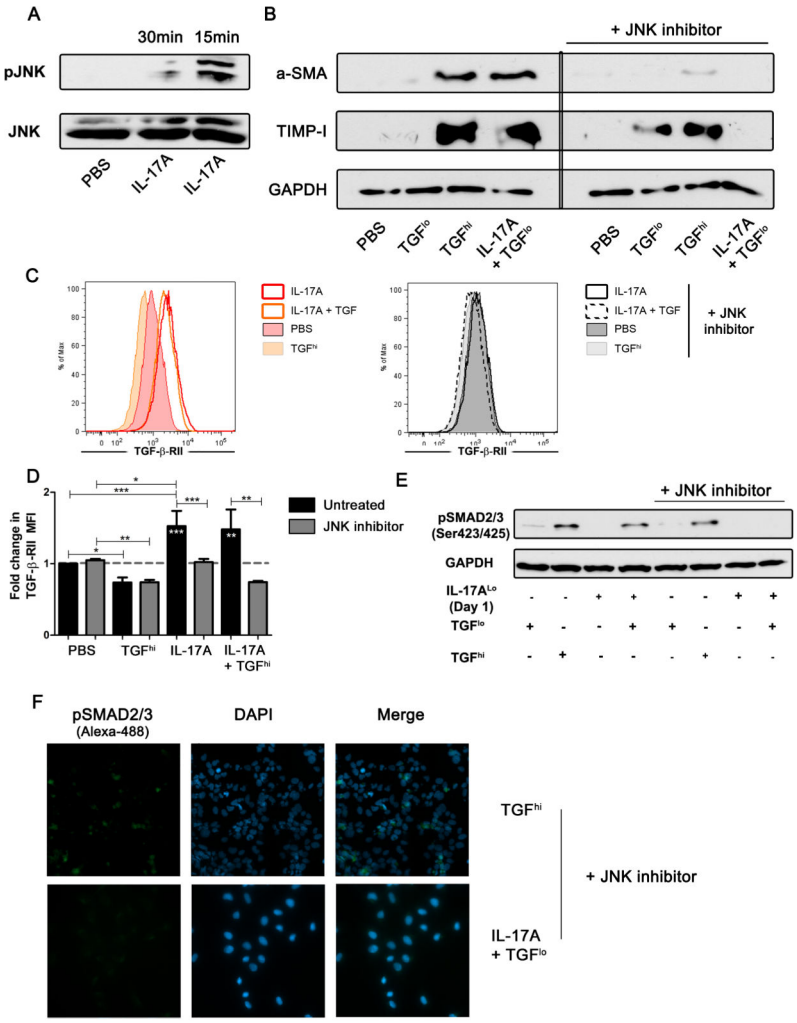

Figure 4. IL-17A enhances TGF-β response of hepatic stellate cells in a JNK-dependent manner

Phosphorylation of JNK was evaluated by western blot after 15–30 min stimulation with IL-17A (A). Protein expression of α-SMA and TIMP-I after 48 h stimulation with TGF-β, TGF-β + IL17A in presence or absence of the JNK inhibitor, SP600125, was evaluated by western blot (B). Cell surface expression of TGF-β-RII was measured by flow cytometry after 48 h stimulation with IL-17A and/or TGF-β in the absence (left panel C) or presence of JNK inhibitor (right panel C). Representative histogram of TGF-β-RII cell surface expression (n=3) after IL-17A and/or TGF-β stimulation (C). Results are display as fold increase of MFI (n=3) (D). Phosphorylation of SMAD2/3 at serine 423/425 was evaluated by western blot after 15 min stimulation with TGF-β in presence of JNK inhibitor (E). Two colors immunofluorescence confocal microscopy was used to observe phosphorylated SMAD2/3 (green, Alexa-488) and nucleus (Blue, DAPI) (F).

Table 1

Primer sequences for qRT-PCR.

Gene	Primer	Accession Number	Sequence	Amplicon Size
r28S	q-28S-Fwd	NR_003287.2	CGAGATTCCCACTGTCCCTA	158bp
	q-28S-Rvs		GGGGCCTCCCACTTATTCTA	
COL1A1	q-COL1A1-Fwd	NM_000088	TCTGCGACAACGGCAAGGTGT	147bp
	q-COL1A1-Rvs		CGACGCCGGTGGTTTCTTGGT	
ACTA2	q-ACTA2-Fwd	NM_001613.2	CCAAGGCCAACCGGGAGAAAATGA	97bp
	q-ACTA2-Rvs		GCATAGAGAGACAGCACCGCCTGG	
TIMP-I	q-TIMP-I-Fwd	NM_003254.2	AATTCCGACCTCGTCATCAGG	123bp
	q-TIMP-I-Rvs		ATCCCCTAAGGCTTGGAACC	